

Targetry for cyclotron production of no-carrier-added cadmium-109 from $^{nat}\text{Ag}(p,n)^{109}\text{Cd}$ reaction

M. Mirzaii¹, M. Sadeghi^{1*}, Z. Gholamzadeh²

¹Agricultural, Medical & Industrial Research School, P.O. Box: 31485/498, Karaj, Iran

²Faculty of Engineering, Research and Science Campus, Islamic Azad University, Tehran, Iran

Background: Solid targets that consist of powder and electrodeposited targets are used commonly to produce radionuclides by accelerators. Since silver is easily electrodeposited in cyanide baths and has a very excellent thermal conductivity, the electrodeposited target is preferable to produce ^{109}Cd . To avoid cracking or peeling of the target during bombardment, it should have a level surface and a good adhesion to substrate. Hence, suitable targetry has extraordinary importance for the interested radionuclide production. **Materials and Methods:** Excitation function of cadmium-109 via $^{nat}\text{Ag}(p,n)^{109}\text{Cd}$ reaction was investigated by using ALICE-91 code. The required thickness of the silver deposit was calculated by SRIM code. Theoretical yield was calculated by means of Simpson numerical integral method. Silver was electrodeposited on copper backing by the cyanide bath. The prepared targets were examined with morphology and thermal shock tests. **Results:** The most favorable beam energy was determined as 15 MeV. The desired thickness was determined to be up to 48 μm ; the theoretical calculated yield was 2.69 $\mu\text{Ci}/\mu\text{A}\cdot\text{h}$. Scanning electron microscope (SEM) photomicrographs and thermal shock tests represented excellent quality of the electrodeposited target. **Conclusion:** The present study suggested a good potentiality of cadmium-109 production by induced proton on electrodeposited silver targets. *Iran. J. Radiat. Res., 2009; 6 (4): 201-206*

Keywords: Excitation function, silver target, cyanide bath, ^{109}Cd , production yield.

INTRODUCTION

Cadmium-109 is a radionuclide that can be used as an X-ray fluorescence source. It has a half-life of 462.6 days and decays by electron capture to $^{109\text{m}}\text{Ag}$ with the emission of a γ -ray with energy of 88.03 keV (3.79%) along with the characteristic X-ray from the K level, with energy of 22.54 keV (102%)⁽¹⁾. This radionuclide can be employed for calibration of detectors and as a tracer to physiological research⁽²⁻⁹⁾. It can also be used in the energy dispersion X-ray fluores-

cence (EDXRF) technique.^(10,11) Cadmium-109 has been applied in physiological research on animals and plants for more than forty years which has provided useful information. This radionuclide can probably be used for inhibition of liver cancerous cells^(12, 13), as well as for tissue imaging with SPECT (single photon emission computed tomography)⁽¹⁴⁾. Additionally, it can be used to investigate the ecosystem⁽¹⁵⁾.

The $^{109}\text{Cd}/^{109\text{m}}\text{Ag}$ generator has been investigated for uses of venogram and angiogram. Since these are usually completed with in a minute after the injection of the radionuclide, the use of ultrashort-lived radionuclides is possible its advantage is the repeating other studies can be performed quickly due to the fact that the radioactivity from a pervious injection would decay away rapidly⁽¹⁶⁾.

The production of ^{109}Cd with a proton beam can be performed by reactions: The product $^{nat}\text{In}(p,x)^{109}\text{Cd}$ ⁽¹⁷⁾ which needs an energy of about 96 MeV, $^{nat}\text{Ag}(d,x)^{109}\text{Cd}$ ⁽¹⁸⁾ with energy 13.4 MeV and $^{nat}\text{Ag}(p,x)^{109}\text{Cd}$,^(19, 20) with an energy range between 14 and 9 MeV, ideal for the cyclotron used in the present study. Accelerator production of ^{109}Cd is largely achieved via nuclear reactions $^{109}\text{Ag}(p,n)^{109}\text{Cd}$ and $^{109}\text{Ag}(d,2n)^{109}\text{Cd}$ which are well suited for low- or medium-energy cyclotrons; such as Cyclone-30 (IBA, Belgium, I_{max} : 300mA, proton E_{max} : 30 MeV). Solid targetry systems on these accelerators are made up of pure copper backing onto which target materials are

*Corresponding author:

Dr. Mahdi Sadeghi, Agricultural, Medical & Industrial Research School, P.O. Box: 31485/498, Karaj, Iran.

Fax: +98 261 4436395

E-mail: msadeghi@nrcam.org

electrodeposited.

One of goals of the present study has been a target preparation which is able to endure high irradiation beams during bombardment. Another important aim has been the ability of the target electrodepositing with any requisite thickness; practically, electrodeposition of any thickness is not possible and it needs a very special bath. Since most of the work directed at replacing cyanide in silver plating has resulted in little more than technical interest, ^(21, 22) the cyanide bath was chosen for targets electroplating with different thickness.

MATERIALS AND METHODS

Excitation functions to ¹⁰⁹Cd production from ^{nat}Ag proton bombardment were calculated using ALICE-91 simulations code. To take full benefit of the related excitation functions and to minimize undesired radionuclide impurities formation, incident proton energy should be achieved using ALICE-91 code. According to SRIM code ⁽²³⁾, the required thickness of target was calculated. SRIM (The Stopping and Range of Ions in Matter) code is a group of programs which calculates the stop and range of ions (up to 2 GeV/amu) into matter using a quantum mechanical treatment of ion-atom collisions (assuming a moving atom as an "ion", and all target atoms as "atoms"). This calculation is made very efficient by the use of statistical algorithms which allow the ion to jump between calculated collisions and then calculate the average the collision results over the intervening gap. During the collisions, the ion and atom have a screened Coulomb collision, including exchange and correlation interactions between the overlapping electron shells. The ion has long range interactions creating electron excitations and plasmons within the target. These are described by including a description of the target's collective electronic structure and interatomic bond structure when the

calculation is made. The charge state of the ion within the target is described using the concept of effective charge, which includes a velocity dependent charge state and long range screening due to the collective electron sea of the target. The physical thickness of the target layer is chosen, for a given beam/target angle geometry, to provide a light-particle exit energy. It is advisable to minimize thickness of the target layer to perform irradiations on 6° target geometry. In cyclotron production of radionuclides, the reaction cross section data play a very important role. One needs full excitation function of the nuclear process to be able to calculate and predict the yield with reasonable accuracy. From a given excitation function, the expected yield of a product for a certain energy range, related to target thickness, can be calculated using the expression:

$$Y = \frac{N_L H}{M} I (1 - e^{-\lambda t}) \int_{E_1}^{E_2} \left(\frac{dE}{d(\rho x)} \right)^{-1} \sigma(E) dE \quad (1)$$

Where Y is the activity (in Bq) of the product, N_L is the Avogadro number, H is the enrichment (or isotope abundance) of target nuclide, M, is mass number of the target element, I, is the projectile current, $dE/d(\rho x)$ is the stopping power ($S_p(E)$), $\sigma(E)$ is the cross section at energy E, λ the decay constant of the product and t the time of irradiation. It is clear that if the projectile energy, beam current and time of bombardment increase, the production yield will be raised.

Theoretical production yield considering the excitation functions, stopping power of proton in the target, and beam current was calculated. To investigate maximum tolerable current, Equation 2 was used. The melting point of silver is 961°C that is utilizable it to irradiate with high proton current. The thermal conductivity coefficient of silver is $K_{Ag}: 4.29 \text{ J.s}^{-1}.\text{cm}^{-1}.\text{K}^{-1}$, so it has an excellent thermal conductivity.

Where a is electroplated silver thick-

$$T_m - T_w = \left(\frac{10.I}{2.k_{Ag}} \cdot \frac{a}{s}\right) + \left(\frac{10.I}{k_{Cu}} \cdot \frac{b}{s} + \frac{5.I}{2.k_{Cu}} \cdot \frac{b}{s}\right) + \left(\frac{15.I}{k_{Cu}} \cdot \frac{c}{s}\right) + \left(\frac{15I}{h.s}\right) \quad (2)$$

ness (cm), b is a copper thickness that stop the 5MeV exit proton (cm), c is rest thickness of backing (cm), s is backing area (cm²) and h is coefficient of thermal conductivity in replacement manner (J/cm².°K.s)

A copper backing was pre-treated and silver was electrodeposited on it with a special cyanide bath. The natural silver (99.99% purity, ¹⁰⁹Ag 48.35%, ¹⁰⁷Ag 51.65%) was purchased from Fluka Company. Silver targets were prepared by DC-CCE (constant current electrolysis) of the metal from alkaline plating solutions. The deposits were tested for thermal shock and morphology.

RESULTS

In order to optimize the ¹⁰⁹Cd production, the effective parameters are investigated as follows:

Proton cross section calculations in natural silver by ALICE-91 code

According ALICE-91 code simulations, to take full benefit of excitation function and to reduce formation of radionuclide impurities, entrance proton energy should be 15 MeV^(24, 25). To take away any isotopic impurity in production solution, the entrance proton energy of 9 MeV was selected (figure 1); selection of 9 MeV entrance energy decrease considerably production yield. Therefore, useful energy range was recognized as 5 to 15 MeV. The physical thickness of the silver layer was chosen in such a way that for a given beam/target angle geometry, the particle exit energy should be 5 MeV. By using enriched ¹⁰⁹Ag, the production yield will be almost twice as much and the ¹⁰⁶Cd stable nuclide will not produce (figure 2).

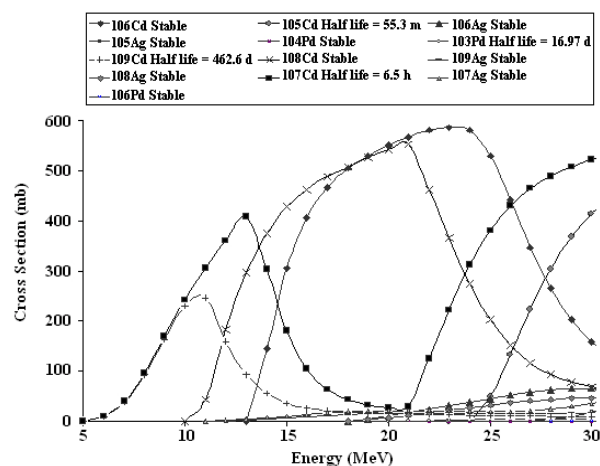


Figure 1. Excitation function of the ^{nat}Ag(p,x) for ¹⁰⁹Cd production using Alice code; ¹⁰⁷Cd (6.5 h), ¹⁰⁶Cd (stable) and ¹⁰⁸Cd (stable) impurities will be produce in energy range of 5 to 15 MeV.

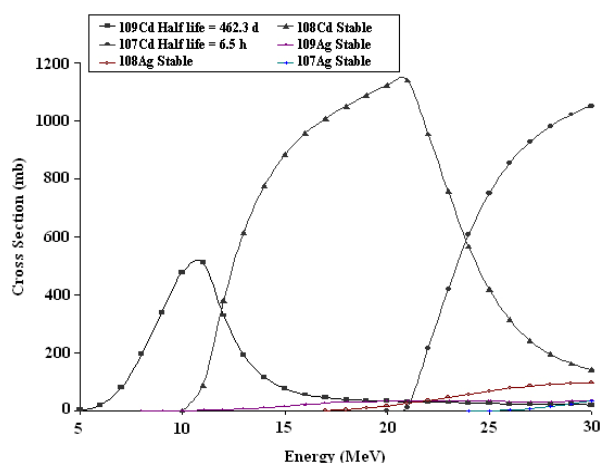


Figure 2. Excitation function of ¹⁰⁹Ag(p,x) for ¹⁰⁹Cd production using Alice code; cross sections will be almost twice as much and the ¹⁰⁶Cd stable nuclide will not produce.

Calculation of the requisite silver thickness by SRIM code

According to the SRIM code, projected range of proton in silver target was calculated; the thickness had to be 352 μm for 90 ° geometry. To minimize the thickness of the silver layer, a 6° geometry is preferred, so the 35 mm thickness of silver recommended for 15 MeV entrance protons leave it with 5 MeV. The 5 MeV protons will produce radiozinc

impurity in copper backing (figure 3). Hence a thickness up to 48 mm was used not only to decrease or remove the radiozinc impurity, but also copper impurity due to washing the target by acid (figure 4).

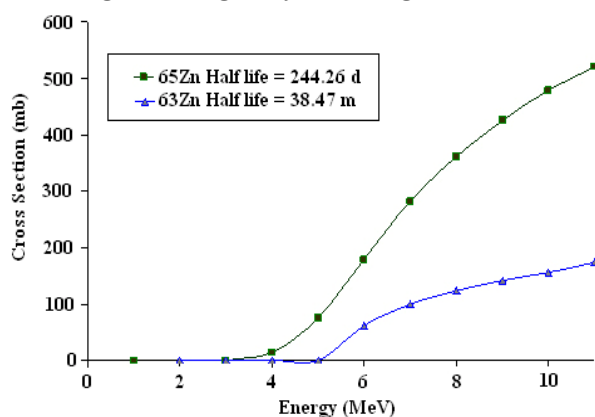


Figure 3. Excitation function of the $^{nat}\text{Cu}(p,xn)^{63/65}\text{Zn}$ using Alice code; radiozinc impurities were produced by exited protons from silver layer with energy up to 5 MeV in copper backing.

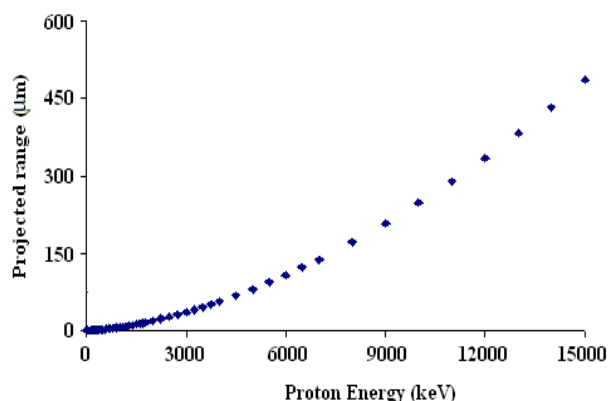


Figure 4. Projected ranges of proton in silver layer; 48 mm thickness was calculated using SRIM code at 15 MeV induced protons for 6° geometry of target/beam.

The yield calculation

The thick target integral yield deduced using the measured cross sections from threshold upto 5 MeV. The yield was calculated by using the Simpson numerical integral as of equation 1.

The obtained results indicate that the yield increases with the increase in the incident energy. However, entrance proton energy more than 15 MeV will not noticeably increase the production yield; furthermore, it will cause problems in cooling of the target (figure 5).

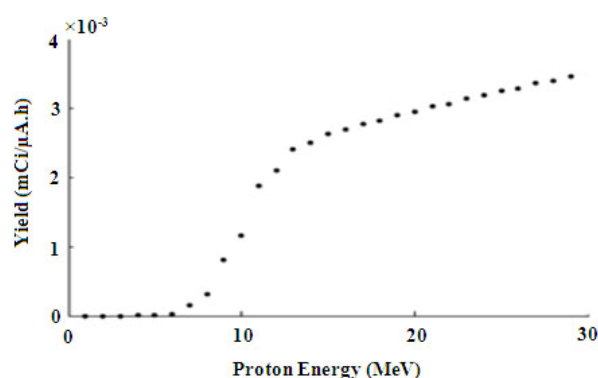


Figure 5. Yield of Cadmium-109 production from $^{nat}\text{Ag}(p,n)$ reaction; the entrance proton energy more than 15 MeV will not noticeably increase the production yield.

Pretreatment of the Cu- backing

Silver is a relatively noble metal; most metals being less noble than silver form immersion deposits on the surface. This tends to happen even when the base metal enters the silver solution hot or live, that is, with an already applied voltage. The inevitable result of this phenomenon is poor adhesion of subsequent deposits. To minimize this effect, it is essential to employ a silver strike coating prior to the main deposit. In this work experiments were carried out on adhesion with and without strike coating. It was noted that if the plating were carried out very rapidly, a good adhesion would be obtained in all electroplated targets without the need for strike coating.

Embrittlement of metals has been recognized for many years, but, some other defects in electrodeposits, such as blistering, cracking, gas pits, peeling off and poor adhesion, may also be related to hydrogen in ways not yet identified. Plating on a dietary or greasy surface inevitably leads to blistering or peeling of deposit. Cathodic cleaning in either acid or alkaline solutions provides large quantities of hydrogen for absorption. (26-29) In all experiments, the substrate surface was cleaned with sandpaper (1000) grade and immersed in the nitric acid bath of 0.3 M. Then, the surface was washed by water and its oil contaminators were removed by mixture of the alkali cleaning powders. Finally, the surface was washed

with acetone.

Electroplating of silver on copper- backing

An electrolysis solution is a volume of about 450 ml and a composition of 5.1 g l⁻¹ AgCN, 5.1 g l⁻¹ KCN, 3 g l⁻¹ Na₂CO₃, while the current between the electrodes is adjusted to 0.05 A. The silver electroplating was performed in constant current. Prior to the silver plating and to ensure a good adhesion, copper plate was cleaned using sandpaper (1000) grade followed by rinsing copper plate with deionized water. The deposits were completely smooth, compact and shiny with 100% current efficiency in acidity between 10-12 and 40°C temperature. Maximum of the deposit thickness obtained from the electroplating solution was 133 mm with suitable adhesion and morphology.

Thermal shock test

The thermal shock tests were carried out by heating the target up to 500 °C (the temperature that the Ag layer can experience during a high current irradiation) for 1 hour followed by submersion of the hot target in cold (8 °C) water. Observation of neither crack formation nor peeling off of the silver layers indicated a good adhesion for the purpose.

Study of thermal conductivity

Silver target thermal conductivity was studied (equation 2); therefore maximum current of beam was determined $I_m = 1248.63 \mu\text{A}$.

Surface morphology examination

A deposit without the dendrite structure formation or not smoothing of the surface is proper for irradiation. Hence, the deposits were examined in morphology by scanning electron microscopy (SEM) technique (using a Joel model JSM 6400 at an accelerating voltage of 20 kV). Neither crack nor dendrite structure were observed on electroplated silver target (figure 6).

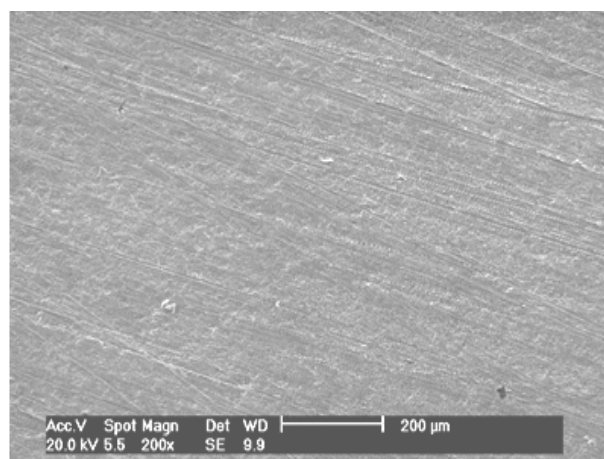


Figure 6. SEM of a silver deposit on the Cu backing grown at a current density of 4.27 mA.cm⁻² from 5.16 gl⁻¹ Ag CN, 5.16 gl⁻¹ KCN, 3 gl⁻¹ Na₂CO₃ solutions, pH=12, 40 °C, 133mm thickness.

DISCUSSION

Making use of natural silver as a target material is more economical than enriched target; greater production yield is only advantage of the enriched target the material utilization, while impurity production is not considerably decreased. The calculated theoretical yield was 2.69 $\mu\text{Ci}/\mu\text{A.h}$ (0.099 MBq/ $\mu\text{A.h}$) using Simpson numerical integral that is in a good agreement with the reported empirical results by Landini *et al.* (0.071 MBq/ $\mu\text{A.h}$)⁽¹⁹⁾ and Wing *et al.* (0.077 MBq/ $\mu\text{A.h}$)⁽²⁵⁾; ALICE-91 code calculations usually have error of about 15-30% (related to nuclear reaction type) comparing experimental data. The most important advantage of silver target preparation by electroplating method on Cu backing is that the target can become cool easily by using water as cooling system inside plows designed back of the substrate. Silver foils as target used by Landini *et al.*⁽¹⁹⁾, Wing *et al.*⁽²⁵⁾ and Paleodimopoulos *et al.*⁽²⁰⁾ could not bear high proton beam because of its low efficiency cooling system. SEM scans and thermal shock tests showed that the prepared targets by cyanide bath can stand high beam current more than 300 mA, because neither cracking nor peeling off was formed on them.

CONCLUSION

Since the silver targets easily withstand a high proton beam, could be irradiated by low-medium energy accelerators even for a long time, ^{109}Cd production is more efficient from $^{\text{nat}}\text{Ag}(\text{p},\text{n})^{109}\text{Cd}$ reaction. Efficient electroplated silver on copper target was successfully tested for high current irradiation for cyclotron production of multi/sub millicurie's amounts of the radionuclide ^{109}Cd .

REFERENCES

1. Browne E and Firestone RB (1996) Table of Radioactive Isotopes. V. S. Shirley (Ed.). John Wiley and Sons. New York.
2. Yoshida S and Ohsugi T (2005) Application of silicon strip detectors to X-ray computed tomography. *Nuclear Instruments and Methods in Physics research A*, **541**: 412-420.
3. Kossert K, Janben H, Klien R, Scheneider MKH, Schrader H (2006) Activity standardization and nuclear decay data of ^{109}Cd . *Applied Radiation and Isotopes*, **64**: 1031-1035.
4. Fleming DEB and Forbes TA (2001) Calibration and characterization of a digital X-ray fluorescence bone lead system. *Applied Radiation and Isotopes*, **55**: 527-532.
5. Sawyer JR, Tucker PW, Blattner FR (1992) Metal-binding chimeric antibodies expressed in *Escherichia coli*. *Applied Biological Sciences*, **89**: 9754-9758.
6. Wolterbeek HTh and Meer AJGM (2002) Transport rate of arsenic, cadmium, copper and zinc in *Potamogeton pectinatus* L.: radiotracer experiments with ^{76}As , $^{109,115}\text{Cd}$, ^{64}Cu and $^{65,69\text{m}}\text{Zn}$. *The Science of the Total Environment*, **287**: 13-30.
7. Din WS and Frazier JM (1985) Protective effect of metallothionein on cadmium toxicity in isolated rat hepatocytes. *Biochem*, **230**: 395-402.
8. Sas KN, Kovacs L, Gombos OZZ, Garab GL, Danielsen HE (2006) Fast cadmium inhibition of photosynthesis in cyanobacteria in vivo and in vitro studies using perturbed angular correlation of γ - rays. *Bio Inorg Chem*, **11**: 725-734.
9. Grawé KP and Oskarsson A (2000) Cadmium in milk and mammary gland in rats and mice. *Springer Berlin / Heidelberg*. **73**: 519-527.
10. Gupta D, Chatterjee JM, Ghosh R, Mitra AK, Roy S, Sarkar M (2007) EDXRF analysis of municipal solid waste using ^{109}Cd source. *Applied Radiation and Isotopes*, **65**: 512-516.
11. Roboco J, Carvalho ML, Marques AF, Frreira FR, Chettle DR (2006) Lead post mortem intake in human bones of ancient populations by ^{109}Cd - based X-ray fluorescence and EDXRF. *Talanta*, **70**: 957.
12. Fritioff A and Greger M (2007) Fate of cadmium in *elodea canadensis*. *Chemosphere*, **67**: 365-375.
13. Moffatt P, Marion M, Denizeau F (1992) Cadmium-2-acetylaminofluorene interaction in isolated rat hepatocytes. *Cell Biology and Toxicology*, **8**: 277-290.
14. Accorsi R, Curion AS, Frallicciardi PR, Lanza C, Lauria A, Mettievier G, Montesi MC, Russo P (2007) Preliminary evaluation of the tomographic performance of the mediSPECT small animal imaging system. *Nuclear Instruments and Methods in Physics research A*, **571**: 415-418.
15. Liu S and Wang WX (2002) Feeding and reproductive responses of marine copepods in South China Sea to toxic and nontoxic phytoplankton. *Marine Biology*, **140**: 595-603.
16. Mansur MS, Mushtaq A, Muhammad A (1995) A $^{109}\text{Cd}/^{109\text{m}}\text{Ag}$ generator. *Radioanal Nucl Chem*, **201**: 205-211.
17. Nortier FM, Mills SJ, Steyn GF (1991) Excitation functions for the production of ^{109}Cd , ^{109}In and ^{109}Sn in proton bombardment of indium up to 200 MeV. *Appl Radiation Isotopes*, **42**: 1105-1107.
18. Peng X, Xianguan L, He F, Li M (1992) Excitation function for $^{107}\text{Ag}(\text{d},2\text{n})^{107}\text{Cd}$, $^{109}\text{Ag}(\text{d},2\text{n})^{109}\text{Cd}$ and $^{109}\text{Ag}(\text{d},\text{p})^{110\text{m}}\text{Ag}$ reactions. *Nucl Instr Meth B*, **68**: 145-148.
19. Landini L and Osso Jr JA (2001) Simultaneous production of ^{57}Co and ^{109}Cd in cyclotron. *J Radioanal Nucl Chem*, **250**: 429-431.
20. Paleodimopoulos E and Paradellis T (1987) Radiochemical purification of cadmium-109 produced by the $^{109}\text{Ag}/\text{p},\text{n}/\text{reaction}$. *J Radioanal Nucl Chem*, **2**: 129-132.
21. Zarkadas GM, Stergiou A, Papanastasiou G (2004) Silver electrodeposition from AgNO_3 solutions containing organic additives. *Journal of Applied Electrochemistry*, **34**: 607-615.
22. Blair A (2002) silver plating. *Metal Finishing*, **100**: 284-290.
23. Ziegler JF, Biersack JP, Littmark U (2003) the code of SRIM—the Stopping and Range of Ions in Matter. *IBM-Research, New York, USA*.
24. Blann M (1991) ALICE-91; Statistical Model Code System with Fission Competition, *RSIC Code Package PSR-146*.
25. Wing J and Huizenga JR (1962) (p,n) cross section of ^{51}V , ^{52}Cr , ^{63}Cu , ^{65}Cu , ^{107}Ag , ^{109}Ag , ^{111}Cd , ^{114}Cd and ^{139}La from 5 to 10.5 MeV. *Physical Rev*, **128**: 280-290.
26. Natarjam S and Krishnan R (1971) *Metal Finishing*, **69**: 51.
27. Fischer J and Weimer DE (1964) Precious Metal Plating. *R. D. Ltd, Teddington, I*.
28. Lowenheim FA (1978) Electroplating fundamentals of surface finishing. *McGraw-Hill*, 258.
29. Durney LJ (1984) Electroplating engineering Hand book, Springer, 58.